

Excitation Spectra in a Heavy-Light Meson-Meson System *

H. R. Fiebig^a (LHPCollaboration)

^aPhysics Department, FIU-University Park, Miami, Florida 33199, USA

A system of two static quarks, at fixed distances r , and two light quarks is studied on an anisotropic lattice. Excitations by operators emphasizing quark or gluon degrees of freedom are examined. The maximum entropy method is applied in the spectral analysis. These simulations ultimately aim at learning about mechanisms of hadronic interaction.

1. INTRODUCTION

While QCD has emerged as the foundation of nuclear physics the question of how the strong hadronic interaction arises from first principles still awaits explanation. Lattice hadron physics holds the most promise for answers. Mechanisms of hadronic interaction may already be studied in systems of hadrons with one heavy, static, quark each. In this case the relative distance between the hadrons is well defined, and studies of the interaction mechanism in terms of intuitive descriptions, like potentials, becomes possible.

In principle, knowledge of the excited states of a two-hadron system allows the construction of an effective interaction. In practice, the extraction of excited states from a lattice simulation is a very difficult problem. The canonical approach is to use plateau fits to effective mass functions. Bayesian inference [1], a pillar in many fields of science, has surprisingly been ignored by the lattice community until only very recently [2]. While the aim of this work is to learn about hadronic interaction mechanisms extraction of the spectral mass density via Bayesian methods emerges as an interesting subject in its own.

2. HEAVY-LIGHT MESON-MESON OPERATORS

Our intention is to test the strengths of different excitation mechanisms, in a two-meson system, as a function of the relative distance r . The

following operators are used

$$\Phi_1(t) = \sum_{\vec{x}, \vec{y}} \delta_{\vec{r}, \vec{x} - \vec{y}} \underbrace{\bar{Q}_A(\vec{x}t) \gamma_5 q_A(\vec{x}t)} \underbrace{\bar{Q}_B(\vec{y}t) \gamma_5 q_B(\vec{y}t)} \quad (1)$$

$$\Phi_2(t) = \sum_{\vec{x}, \vec{y}} \delta_{\vec{r}, \vec{x} - \vec{y}} U_{P; AA'}(\vec{x}t, \vec{y}t) U_{P; B'B}^\dagger(\vec{x}t, \vec{y}t) \underbrace{\bar{Q}_A(\vec{x}t) \gamma_5 q_B(\vec{x}t) \bar{Q}_{B'}(\vec{y}t) \gamma_5 q_{A'}(\vec{y}t)}. \quad (2)$$

The operator Φ_1 represents a product of two local pseudo scalar mesons. The fields Q, q denote heavy and light quarks, respectively. Indices A, A', B, B' mean color, and U_P are link variable products along straight paths P . In Φ_2 color singlets, i.e. mesons, spread across a distance r . Excitations due to these nonlocal operators involve gluon exchange degrees of freedom. In contrast, Φ_1 excitations involve states where the mesons mostly communicate via $\bar{q}q$ exchange, at large r . Diagrammatic representations of diagonal correlator matrix elements $C_{ii}(t, t_0) = \langle \hat{\Phi}_i^\dagger(t) \hat{\Phi}_i(t_0) \rangle$ shown in Fig. 1 illustrate these points. We will loosely refer to Φ_1 and Φ_2 as emphasizing gluon and quark degrees of freedom (d.o.f.).

3. TECHNICAL LATTICE ISSUES

Light-quark propagators are computed from random Z_2 -source estimators [3] which are non-zero on time slice t_0 only. Heavy-quark propagators are treated in the static approximation, i.e. as link products along straight temporal paths.

*This material is based upon work supported by the National Science Foundation under Grant No. PHY-0073362.

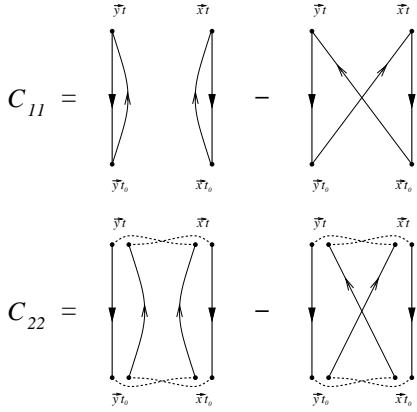


Figure 1. Diagrammatic impressions of the correlators C_{11} and C_{22} representing quark and gluon exchange degrees of freedom, respectively.

Gaussian smearing of the quark fields and APE fuzzing of the gluon field links is applied.

Simulations are done on a $L^3 \times T = 10^3 \times 30$ anisotropic lattice with a (bare) aspect ratio of $a_s/a_t = 3$. We use the tadpole improved gauge field action of [4] with $\beta = 2.4$. This corresponds to a spatial lattice constant of $a_s \simeq 0.25\text{fm}$, $a_s^{-1} \simeq 800\text{MeV}$. The (quenched) anisotropic Wilson fermion action is augmented with a clover action limited to spatial planes. Only spatial directions are improved with renormalization factors $u_s = \langle \square \rangle^{1/4}$, while $u_t = 1$ in the time direction. The Wilson hopping parameter $\kappa = 0.0679$ leads to the mass ratio $m_\pi/m_\rho \simeq 0.75$.

4. SPECTRAL DENSITY

For an operator combination $\Phi_v = v_1 \Phi_1 + v_2 \Phi_2$ the correlation function

$$C_v(t, t_0) = \langle \hat{\Phi}_v^\dagger(t) \hat{\Phi}_v(t_0) \rangle = \quad (3)$$

$$= \sum_{n \neq 0} |\langle n | \hat{\Phi}_v(t_0) | 0 \rangle|^2 e^{-\omega_n(t-t_0)} \quad (4)$$

has forward ($\omega_n > 0$) and backward ($\omega_n < 0$) going contributions on a periodic lattice. We normalize those differently, defining

$$\exp_T(\omega, t) = \Theta(\omega) e^{-\omega t} + \Theta(-\omega) e^{+\omega(T-t)}, \quad (5)$$

the spectral model

$$F(\rho_T | t, t_0) = \int_{-\infty}^{+\infty} d\omega \rho_T(\omega) \exp_T(\omega, t - t_0) \quad (6)$$

is then expected to fit the lattice correlators. Specifically, the requirement $F(\rho_T | t, t_0) = C_v(t, t_0)$ leads to a sum of discrete δ -peaks for the spectral density

$$\rho_T(\omega) = \sum_{n \neq 0} \delta(\omega - \omega_n) |\langle n | \hat{\Phi}_v(t_0) | 0 \rangle|^2 \times \quad (7)$$

$$[\Theta(\omega_n) + \Theta(-\omega_n) e^{-\omega_n T}].$$

The peak-like signature should survive in the discretized form of (6)

$$F(\rho | t, t_0) \simeq \sum_{k=K_-}^{K_+} \rho_k \exp_T(\omega_k, t - t_0), \quad (8)$$

where $\Delta\omega$ is a suitable interval, $\omega_k = \Delta\omega k$, and $\rho_k = \Delta\omega \rho_T(\omega_k)$.

From the Bayesian point of view the spectral weights $\rho_k, k = K_- \dots K_+$, as well as the values $C_v(t, t_0), t = 0 \dots T-1$, of the correlation function are stochastic variables, ρ and C , subject to certain probability distribution functions. The conditional probability $\mathcal{P}[C \leftarrow \rho]$ of C , given ρ , is known as the likelihood function. For a large number of measurements we have $\mathcal{P}[C \leftarrow \rho] \propto e^{-\chi^2/2}$, see [1], where

$$\chi^2 = \sum_{t_1, t_2} [C_v(t_1, t_0) - F(\rho_T | t_1, t_0)] \times \quad (9)$$

$$\Gamma_v^{-1}(t_1, t_2) [C_v(t_2, t_0) - F(\rho_T | t_2, t_0)]$$

is the usual χ^2 -distance between the data and the model, and $\Gamma_v^{-1}(t_1, t_2)$ denotes the inverse covariance matrix [5]. It accounts for the statistical dependence of correlator data between time slices. Assuming minimal information (in the sense of [6]) about ρ the Bayesian prior probability is $P[\rho] \propto e^{\alpha S}$ where α is a parameter and

$$S[\rho] = \sum_k \left(\rho_k - m_k - \rho_k \ln \frac{\rho_k}{m_k} \right) \quad (10)$$

is the entropy relative to m , the latter being called the default model [1]. By virtue of Bayes' theorem [7] the so-called posterior probability is

$$\mathcal{P}[\rho \leftarrow C] = \mathcal{P}[C \leftarrow \rho] P[\rho] / P[C] \propto e^{-W[\rho]}, \quad (11)$$

for a given C , where W is defined as

$$W[\rho] = \chi^2/2 - \alpha S. \quad (12)$$

The most likely ρ is obtained by minimizing $W[\rho]$. The method of choice [2], so far, has been singular value decomposition (SVD). Indeed, the functional $W[\rho]$ has a unique minimum [1]. Stochastic methods, however, seem more in tune with the Bayesian perspective. In this spirit we have employed simulated annealing to obtain the spectral density. The corresponding partition function is

$$Z_W = \int [d\rho] e^{-\beta_W W[\rho]}. \quad (13)$$

A Metropolis algorithm was used with local updates $\rho_k \rightarrow x\rho_k$ where x is a random deviate with distribution $p_2(x) = xe^{-x}$. For the annealing schedule a power law $\beta_W(n) = (\beta_1 - \beta_0)(n/N)^\gamma + \beta_0$ turned out to be suitable.

5. RESULTS

We have explored the α -dependence of ρ using an artificial (mock) data set compiled from eigenvalues of the 2×2 correlation matrix $C_{ij}(t, t_0)$. Cooling averages were taken during the last 200, of $N = 2200$, cooling steps during which the final β_W was kept constant. For tuning purposes it is useful to monitor the entropy load

$$S/W := \frac{\langle -\alpha S \rangle_{\beta_W \rightarrow \infty}}{\langle W \rangle_{\beta_W \rightarrow \infty}}. \quad (14)$$

At constant default model $m = 10^{-12}$ the entropy weight α was varied over 15 orders of magnitude. Two examples are shown in Fig. 2. Remarkably the gross structure of the spectral density remains stable across 8 orders of magnitude of α . The second pair of frames in Fig. 2 marks a kind of critical point α_S , beyond which the annealing action W becomes entropy dominated, the onset of ignoring the evidence $\mathcal{P}[C]$. This results in a smoothing of the contours of the large- ω peak, see Fig. 2. Even so, the fit to the correlation function is not greatly affected. We found that a good criterion for choosing the entropy weight parameter α is to tune S/W to about $\leq 10^{-2}$. As is evident from Tab. 1, near this value the linear relationship between S/W and α begins to break down.

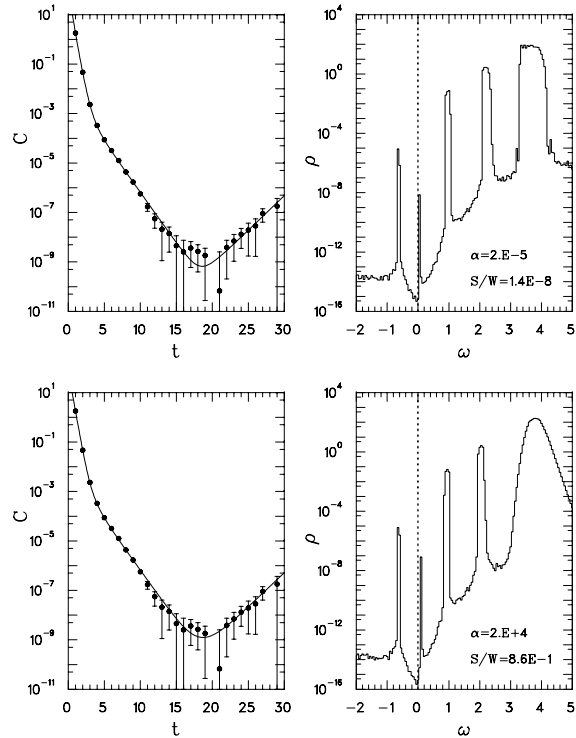


Figure 2. Entropy weight dependence. Correlators and spectral densities for an artificial data set, at relative distance $r = 1$ and constant default model $m = 10^{-12}$, for $\alpha = 2 \times 10^{-5}$ and $2 \times 10^{+4}$, respectively.

To explore the default model dependence the correlation function C_{11} of the local meson-meson operator (1) was analyzed for a series of constant models m . The results for two values, $m = 10^{-12}$ and $m = 1.0$, are shown in Fig. 3. Different entropy weight parameters, $\alpha = 100$ and 1000 , were chosen such that the entropy load S/W is about the same. Increasing m by twelve orders of magnitude changes ρ at the high- ω end. In that region spectral peaks are apparently not supported by the data. Thus the spectral density tends towards the default model. Again, absence of information leads to a smoother curve. Note that the change in ρ for $\omega > 3$ is numerically inconsequential due to the presence of large peaks, also, the gross structure of the spectral function is sta-

Table 1

The entropy load S/W for some entropy weight parameters α . Note the linear relationship in the region $\alpha \leq 2 \times 10^{+1}$.

α	S/W
2×10^{-5}	1.4×10^{-8}
2×10^{-2}	1.4×10^{-5}
$2 \times 10^{+1}$	1.4×10^{-2}
$2 \times 10^{+4}$	8.6×10^{-1}

ble against changing m . On the other hand, the micro structure of like peaks in Fig. 3 differs noticeably.

It is well known that the functional (12) has a unique absolute minimum [1]. Any start configuration used in the annealing process will result in a final configuration ρ that is merely close to the absolute minimum, since $\beta_W < \infty$. Then, which features of ρ are independent of the start configuration? Figure 4 shows two spectral functions obtained from a cold start at $m = 10^{-12}$ and a random start. There is a main and a secondary peak (1' and 1''). Repeated computation of ρ with varying random starts and annealing schedules shows that the two-peak feature is stable, thus being a property of the data. We have looked at peak volumes and energies

$$Z_n = \int_{\delta_n} d\omega \rho_T(\omega) = |\langle n | \hat{\Phi}_v(t_0) | 0 \rangle|^2 \quad (15)$$

$$E_n = Z_n^{-1} \int_{\delta_n} d\omega \rho_T(\omega) \omega \quad (16)$$

where $\delta_n = \{\omega | \omega \in \text{peak } \#n\}$. In Tab. 2 there are listed the peak volumes obtained from a sample of 4 starts (1 cold, 3 random), and the averages (ave) and standard deviations (sig). Assuming that the spectral density comprises two distinct states, 1' and 1'', the variances of $Z_{1'}$ and $Z_{1''}$ are ≈ 10 . Their combined volume $Z_{1' \cup 1''}$ however has a variance less by one order of magnitude. Peak splits, and also spikes, can be caused by imperfect lattice data. In this light, interpreting Fig. 4 in terms of only one physical state, $1 = 1' \cup 1''$, as opposed to two, $1 = 1'$ and $2 = 1''$, is a possibility. More analysis work will be needed to decide this matter.

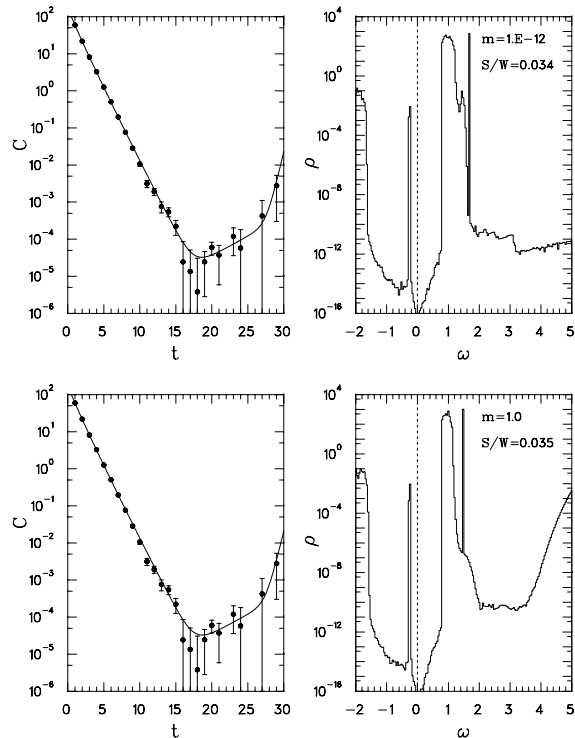


Figure 3. Default model dependence. Correlators of the two-meson operator Φ_1 at relative distance $r = 2$. The spectral densities are obtained with constant default models of $m = 10^{-12}$ and $m = 1.0$, respectively, at constant entropy load S/W .

Among the features of ρ that are computable via spectral analysis are low- ω moment integrated quantities, like the peak volume Z_n and energy E_n , for some state n . These are interesting observables because they may reveal aspects of the physics of hadronic interaction. For example, the relative strength of excitations due to operators Φ_2 versus Φ_1 is measured by $\zeta = \ln(Z_2/Z_1)$, in a normalization independent way. We have plotted ζ in Fig. 5 as a function of the relative meson-meson distance r . As r decreases Φ_2 -type excitations gain strength over Φ_1 -type excitations. In view of (1), (2), and Fig. 1 we may say that gluon exchange degrees of freedom move to dominate quark exchange d.o.f. at small r . We consider Fig. 5 a preliminary result, a more detailed anal-

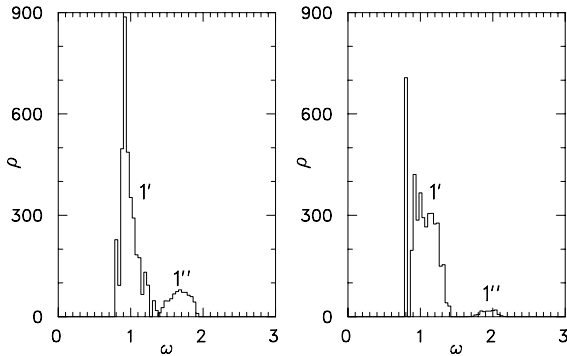


Figure 4. Spectral densities from a cold and a random start, for Φ_1 at $r = 2$, also see Tab. 2.

Table 2

A possible peak split. With 4 different annealing starts the peak volume (15) fluctuates between peaks $1'$ and $1''$.

Start	$Z_{1'}$	$Z_{1' \cup 1''}$	$Z_{1''}$
1	142.0	170.9	28.9
2	162.9	167.9	5.0
3	155.4	170.2	14.8
4	141.1	171.0	29.9
ave	150.3	170.0	19.7
sig	9.2	1.3	10.4

ysis is in progress. Possibly, in the chiral limit, level crossing of ϵ_2 and ϵ_1 in Fig. 5 may occur [8].

6. CONCLUSION

Studies of hadronic interaction require extracting excited states from lattice simulations. Bayesian inference proves a superior tool compared to standard plateau methods. Using an entropic Bayesian prior integrated quantities, like the excitation strengths and energies of certain states, can be reliably computed. The excitations of a heavy-light meson-meson give insight into aspects of strong interaction physics. At the current lattice parameters, quark degrees of freedom still dominate the physics of hadronic interaction.

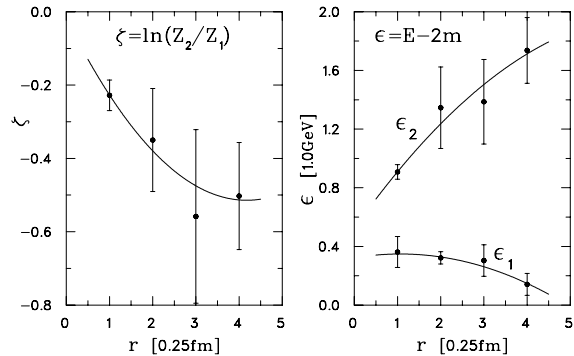


Figure 5. Normalization independent excitation strength ratio ζ of gluon versus quark exchange degrees of freedom as a function of the relative meson-meson distance r (left). Also shown are the corresponding energy shifts $\epsilon_{1,2}$ compared to the mass $2m$ of two noninteracting mesons (right). The error bars reflect annealing start standard deviations.

REFERENCES

1. M. Jarrell and J.E. Gubernatis, Phys. Rep. 269 (1996) 133.
2. Y. Nakahara, M. Asakawa, and T. Hatsuda, Nucl. Phys. B (Proc. Suppl.) 83 (2000) 191.
3. S.J. Dong and K.-F. Liu, Phys. Lett. 328 B (1994) 130.
4. C.J. Morningstar, and M.J. Peardon, Phys. Rev. D 60 (1999) 034509.
5. S. Brandt, *Statistical and computational methods in data analysis*. (North-Holland, New York, 1976).
6. C.E. Shannon and W. Weaver, *The Mathematical Theory of Communication*, Univ. of Illinois Press, Urbana, 1949.
7. G.E.P. Box and G.C. Tiao, *Bayesian inference in statistical analysis* (Addison-Wesley, Reading, 1973).
8. H.R. Fiebig, H. Markum, K. Rabitsch, and A. Mihály, Few Body Syst. 29 (2000) 95.